



# An experimental study of the relationship between cutting efficiency and cuttings size in rock cutting using a PDC cutter

Huihui Hou<sup>1</sup> · Zhong Liu<sup>2</sup> · Hongwu Zhu<sup>1</sup> · Zhenquan Wang<sup>3</sup> · Zhuo Yin<sup>1</sup>

Received: 23 August 2020 / Accepted: 5 April 2021 / Published online: 23 April 2021  
© The Brazilian Society of Mechanical Sciences and Engineering 2021

## Abstract

Rock cutting efficiency is the most common parameter used to evaluate the performance of polycrystalline diamond compact (PDC) bits. Many studies have shown that cuttings size might be used to evaluate rock breaking efficiency; however, there are few quantitative studies of the relationship between rock cutting efficiency and cuttings size in rock cutting when a PDC bit is used. Several linear cutting tests were conducted to explore the relationship between the mechanical specific energy (MSE) and cuttings size to solve this problem. The cuttings size distributions were also discussed. Then, the coarseness index (CI) was selected as the most appropriate indicator of cuttings size and its relationship with the MSE was investigated. In addition, rock cutting tests based on the Taguchi method were conducted to analyze cutting parameters such as the depth of cut (DOC), the back rake angle ( $\theta$ ) and the cutting speed ( $v$ ) effects on the CI and MSE. The contribution of each parameter to the response was obtained. The results show that the distribution of cuttings size conforms to the Rosin–Rammler equation, and there is a significant relationship between the MSE and cuttings size. The MSE decreases with increased cuttings size, furthermore, the relationship between the MSE and the CI could be described by an exponent function. The Taguchi experiment results show that DOC and  $\theta$  have significant impacts: the CI value increases with increased DOC, and the CI increases slightly with increased  $\theta$ . The most influential factor on the CI is the DOC, followed by  $\theta$ . However, within the range of experiments, the cutting speed has an insignificant effect on the CI value. This work is highly pertinent to better understanding of the relationship between rock cutting efficiency and cuttings size in rock cutting using a PDC cutter.

**Keywords** PDC cutter · Cutting efficiency · Cuttings size distribution · Coarseness index · Mechanical specific energy

## 1 Introduction

Since PDC bits were introduced in the early 1970s, PDC bits have become the most widely used bits in the petroleum industry because of advantages such as no rotating parts, high rate of penetration (ROP) and durability [1–3]. With

the development of oil and gas resource exploration, higher quality PDC bits are required, and the design of a better PDC bit has become a popular and important research topic. A better understanding of the interaction mechanism between PDC cutter and rock during the drilling process is needed to improve the design. Many researchers have identified the cutting efficiency prediction of PDC cutter as the most straightforward performance indicator [4–7].

The MSE, a widely used parameter to evaluate the efficiency of rock cutting by PDC cutters, is the energy to break a unit volume of rock. A larger MSE means more energy is used, and thus, cutting efficiency is lower [8, 9]. However, evaluation of the cutting efficiency using the MSE is time consuming and difficult. For this reason, a better approach is needed to evaluate the rock cutting efficiency. Many scholars have conducted theoretical and experimental research in this area and found a strong correlation between cutting efficiency and cuttings size. Thomas and Steven developed an analytical model to describe the dependence of the specific

---

Technical Editor: Celso Kazuyuki Morooka.

---

✉ Hongwu Zhu  
2016314008@student.cup.edu.cn

<sup>1</sup> College of Mechanical and Transportation Engineering, China University of Petroleum-Beijing, Changping, Beijing 102249, China

<sup>2</sup> Faculty of Engineering, China University of Petroleum-Beijing at Karamay, Karamay, Xinjiang 834000, China

<sup>3</sup> Faculty of Petroleum, China University of Petroleum-Beijing at Karamay, Karamay, Xinjiang 834000, China

grinding energy on the material removal regime and conducted several experiments, the results of which showed that the specific grinding energy remained relatively constant for ductile-regime grinding but decreased following a power-law relationship with an increasing material removal rate for brittle-regime grinding [10]. Rock cutting exhibits a similar phenomenon, and it has drawn a large amount of attention from researchers [11–14]. Richard et al. experimentally found that ductile-mode cutting was accomplished by volumetrically deforming the material (powder-like cuttings) ahead of the cutter while brittle-mode cutting was characterized by chip-pings formed by macroscale fracturing (chunk-like cuttings), as shown in Fig. 1. They also found that the ductile-dominated mode needed more energy to break a unit volume of rock than the brittle-dominated mode [11, 12]. He et al. conducted a series of experiments to study the effects of the cutting parameters on the MSE and developed a new method to identify the critical failure mode transition depth in rock cutting [15]. These studies indicated that the existence of two failure modes in rock cutting demonstrates the correlation between cutting efficiency and cuttings size, but more quantitative research is needed to better understand this problem.

Because the cuttings produced during rock cutting vary in size, providing a reasonable index to quantify the cuttings size is a precondition to doing the quantitative research on the relationship between cutting efficiency and the cuttings size. To solve this problem, many studies have shown that there is a strong inverse correlation between the MSE and cuttings size indicators, such as the coarseness index (CI), mean grain size, and absolute grain size ( $r_e$ ) [16–18]. Zhen et al. conducted a series of linear cutting tests with the PDC cutter and concluded that the higher the powder-like cuttings mass fraction was, the larger the MSE needed to break the rock [19]. Hughes et al. carried out theoretical studies on the effect of cuttings size on the MSE or cutting efficiency, they developed a mathematical model to describe the relationship between the MSE and the cuttings size:

$$dE_S = -dD \frac{C}{D^n} \quad (1)$$

where  $E_S$  is the MSE;  $D$  is the average diameter of the cuttings and  $C$  is a coefficient [20, 21]. Roxborough and Rispin defined the coarseness index (CI) as the comparative size

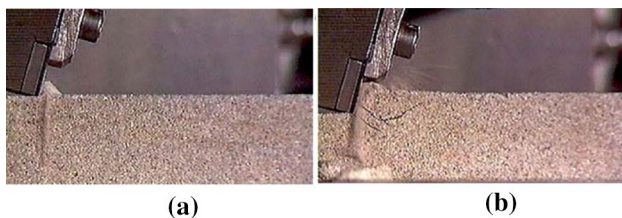


Fig. 1 Rock failure in **a** ductile mode, **b** brittle mode [15]

distribution of the cut rocks, and thus, the numerical CI is the sum of the cumulative weight percentages retained in each sieve used. They noticed that CI values followed a reverse trend to the MSE in rock cutting tests [22]. Tuncdemir et al. performed a large set of cutting tests with different cutting tools on different kinds of rocks and developed an inverse relationship between the MSE and CI:

$$MSE = kCI^n \quad (2)$$

where  $k$  is a coefficient related to the rock strength and cutting tool parameters, and  $n$  is a coefficient related to the sharpness of the cutting tool [21]. Heydari et al. analyzed nine field testing datasets to examine the relationship between various tunnel boring machine (TBM) operational factors, its performance and the muck geometry. They found that there was a strong relationship between the MSE and three muck size indicators: the CI, the mean particle size, and  $r_e$  [23]. In this study, the CI was selected to analyze the cuttings size and investigate its relationship with the MSE because it is easy to calculate.

The effect of cutting parameters on cutting efficiency is another active research area. Researches on critical failure mode transition depth in rock cutting have shown that within the ductile failure mode (in shallow cutting), the average MSE input in a rock cutting test is larger than within the brittle failure mode (in deep cutting). The deeper the cut, the higher the large cuttings mass fraction is, and the smaller the MSE needed [16–19, 24]. With a series of experiments, Rajabov et al. showed that the back rake angle has substantial effects on the MSE [25]. Menezes built a numerical simulation model of rock cutting and conducted several simulations, which showed that the back rake angle has a significant influence on the fragment morphology during rock cutting, and the size of the chip was largest at an angle of  $+15^\circ$ , followed by  $0^\circ$  and  $-15^\circ$  [26]. However, there is no general conclusion regarding the effect of cutting speed on the cutting process [19]. Some other parameters affect the MSE, such as the confining pressure, the shape of PDC cutter, and the rock pore pressure, have been studied by many researchers [27–29]. All these parameters can influence the ROP in oil drilling [30]. However, in this paper, the back rake angle of PDC cutter (determined by bit design), the cutting speed (determined by the rotation speed of bit) and the depth of cut (determined by the weight on bit, the bit design, formation conditions and many other field factors) were used to investigate their effect on cuttings size by laboratory experiments. Less quantitative research has been carried out on the effects of cutting parameters on cuttings size, for this reason, this research will address this topic.

From the results obtained so far, there can be no doubt about the strong correlation between the MSE and the cuttings size. However, quantitative studies of the relationship between rock cutting efficiency and cuttings size during rock cutting by a PDC cutter are few, thus, further research is needed in this field. In addition, research on the effects of cutting parameters on cuttings size is in scant supply. Several linear rock cutting tests were conducted in this work to help fill these gaps. The cutting forces were recorded, and cuttings were collected for sieving. Finally, a mathematical model of the relationship between cuttings size and MSE was established, and the cuttings size distribution was discussed. Moreover, a Taguchi's L25 OA was used to study the effects of the cutting parameters (DOC,  $\theta$ , and  $\nu$ ) on the cuttings size and the MSE. These research results will promote a better understanding of the rock breaking mechanism.

## 2 Experimental setup and data acquisition

### 2.1 Experimental equipment and consumables

The linear rock cutting tests were conducted on a modified multi-purpose machine, as shown in Fig. 2. This experimental system includes a moving stage (with a maximum moving speed of 30 mm/s and a minimum moving speed of 2 mm/s), a rock sample holder, a cutter holder with several adjustable rake angles, a 3-D force sensor, a DOC adjustment device with an accuracy of 0.1 mm, a DC power supply and a data acquisition card (maximum sampling frequency: 100 kHz).

The rock sample used in this research is limestone and its physical parameters are obtained using rock mechanical tests such as the uniaxial compression test and the Brazilian tensile test, as shown in Fig. 3. The results of these tests are given in Table 1. Due to the limitation of the equipment, rock samples used in these tests were machined into 100 × 100 × 70 mm

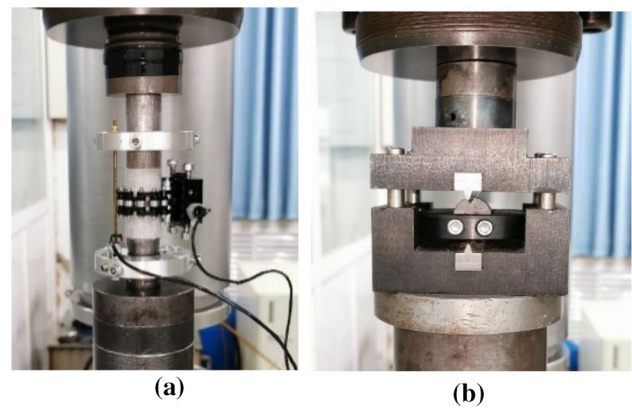


Fig. 3 Rock mechanical tests a Uniaxial compression test, b Brazilian tensile test



Fig. 4 The electronic balance and sieves used in the tests

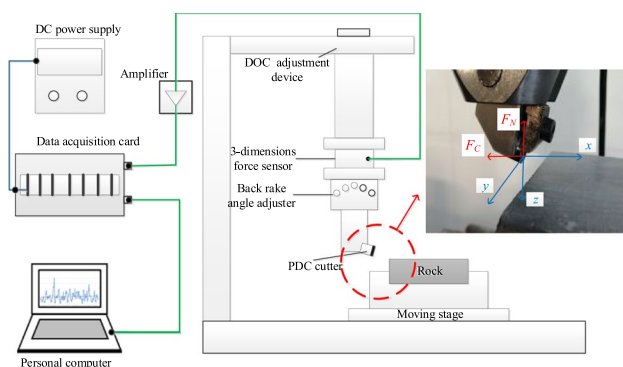


Fig. 2 The linear rock cutting device and the reference frame

blocks. Moreover, the surface flatness and parallelism of the rock samples were strictly controlled to ensure the accuracy of the results.

In this research, a typical  $\Phi$  13.4 mm cylindrical PDC cutter without chamfer was selected as the cutting tool. The PDC cutter should be changed after a few tests to ensure the cutter kept sharp, which improves the accuracy of the rock cutting tests results. In addition, five different sieves (20, 40, 60, 80, 100 mesh) and an electronic balance (value of a scale division: 0.1 mg) were used to determine the size distribution of the collected cuttings (Fig. 4).

Table 1 Mechanical properties of limestone

Density (Kg/m <sup>3</sup> )	Uniaxial compressive strength (MPa)	Brazilian tensile strength (MPa)	Young's modulus (GPa)	Poisson's ratio
2714	116.16	8.39	35.96	0.15

### 2.2 Calculation of the MSE and CI

As the PDC cutter with back rake angle  $\theta$  breaks the limestone at speed  $v$ , the forces applied to the PDC cutter can be decomposed into two orthogonal forces: cutting force ( $F_C$ ) and thrust force ( $F_N$ ), as shown in Fig. 5. Since the depth of cut is constant in a test, the input work due to the thrust force is zero, and only the cutting force was considered during the calculation of the MSE. Moreover, after several cutting tests, some rocks on the side of the cutting trajectory were broken, and in order to calculate the volume of rock broken

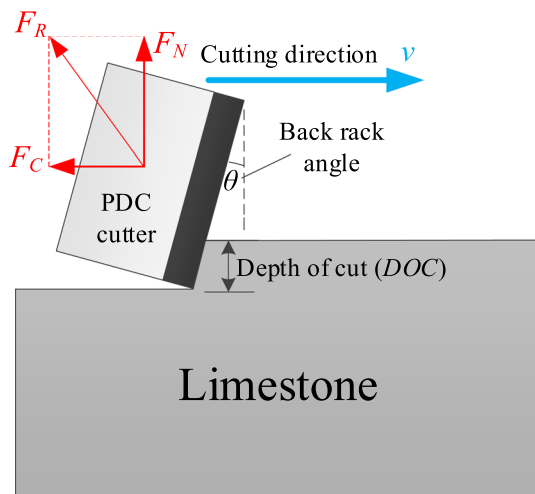


Fig. 5 Forces applied to the PDC cutter

Table 2 An example of CI calculation

Sieves (mesh)	Cumulative weight ( $M_i$ /g)	Cumulative weight percentage (%)
20	0.1244	25.21
40	0.2652	53.74
60	0.3133	63.49
80	0.3358	68.04
100	0.3513	71.19
> 100	0.4935	100
Total weight ( $M$ /g)	0.4935	CI ( $\Sigma$ )=381.67

Table 3 Experimental arrangements

Cutter	Cutting parameters	
Typical $\Phi$ 13.4 mm PDC cutter	Cutting speed ( $v$ , mm/s)	16
	Back rake angle ( $\theta$ , °)	5, 10, 15, 20, 25
	Depth of cut ( $DOC$ mm)	0.1, 0.2, 0.3, 0.4, 0.5, 0.8, 1.2, 1.6, 2.0

accurately, the cuttings were collected and weighed. Then, the MSE could be calculated using the following equation:

$$MSE = \frac{F_C \times L \times \rho}{M} \tag{3}$$

where  $F_C$  is the mean cutting force,  $L$  is the cutting length,  $\rho$  is the density of the rock and  $M$  is the weight of the cuttings.

According to Wang [7], Roxborough [21] and Tuncdemir [22], CI is the sum of the cumulative weight percentages retained in each sieve, and the size of sieves used has a definite effect on its value. Therefore, a series of sieving tests were conducted until we had selected the appropriate sieve sizes for the cuttings. In this work, the CI was calculated using Eq. (4) and an example CI calculation is given in Table 2 ( $DOC=0.5$  mm,  $\theta=5^\circ$ ,  $v=4$  mm/s).

$$CI = \sum_{i=1}^N \frac{M_i}{M} \tag{4}$$

where CI is the coarseness index,  $N$  is the number of sieves used in the tests,  $M_i$  is the cumulative weight of cuttings retained in sieve  $i$ , and  $M$  is the total weight of cuttings.

## 3 Rock cutting tests with different cutting parameters

### 3.1 Experimental procedures

Many cutting tests with different cutting efficiencies are necessary to study the quantitative relationship between the MSE and cuttings size. In this research, cutting efficiency was changed by changing the depth of cut and back rake angle. Since two different failure modes exist during rock cutting progress, it is necessary to carry out rock cutting tests with shallow and deep cuts to avoid the rock failure mode affecting on the relationship between the MSE and cuttings size. In addition, all rock cutting tests in this section were conducted at a constant cutting speed of 16 mm/s. Experimental design parameters are given in Table 3. After each test, the cuttings were collected, separated into groups by size, and weighed. The MSE, the representative of the cutting efficiency, was calculated by the method outlined in Sect. 2.2.

### 3.2 Results and discussion

#### 3.2.1 Distribution of cuttings size

After collecting the cuttings sample, the cuttings were separated into six groups based on their sizes, as shown in Fig. 6. The large cuttings (>0.2 mm) are flat, but the powder-like cuttings (<0.15 mm) are too small for the shape to be determined with naked eye. This paper will focus on cuttings size, so no further study of the cuttings shape was done. In 1933, Rosin and Rammler developed an equation to analyze the laws governing the fitness of powdered coal [23, 31], as given in Eq. (5):

$$R = 100\exp\left(-\left(\frac{r_c}{r_e}\right)^{n_b}\right) \tag{5}$$

where  $R$  is the cumulative fraction of cuttings by weight retained on the sieve that of mesh size  $r_c$ ,  $r_e$  is the absolute grain size,  $n_b$  is a constant describing the uniformity of the cuttings. In double logarithmic coordinates, Eq. (5) can be expressed as Eq. (6):

$$\ln \ln (100/R) = n_b \ln r_c - n_b \ln r_e \tag{6}$$

where  $n_b \ln r_e$  is a constant and Eq. (6) is a straight line in log–log coordinates, hence,  $n_b$  and  $r_e$  can be obtained by a linear fit. The cuttings size distribution data collected from rock cutting tests are shown in “Appendix,” and the fitting results according to Eq. (6) are shown in Fig. 7. It shows a statistically significant correlation between  $\ln \ln (100/R)$

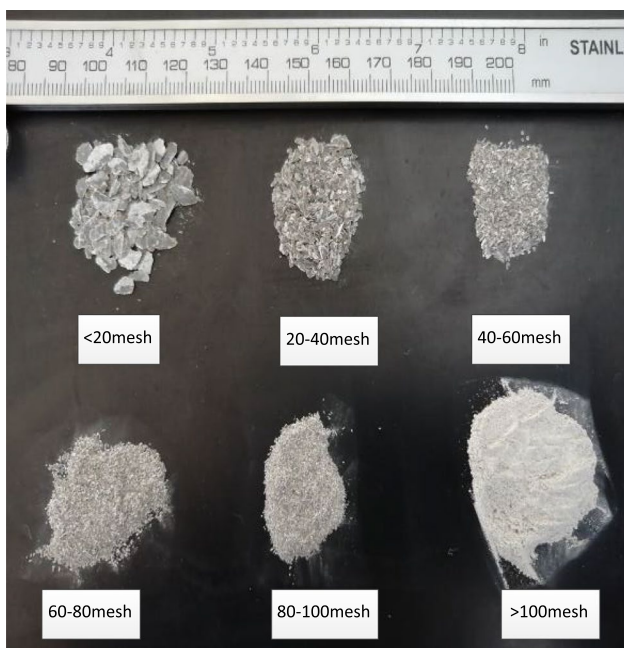


Fig. 6 The cuttings collected from rock cutting tests

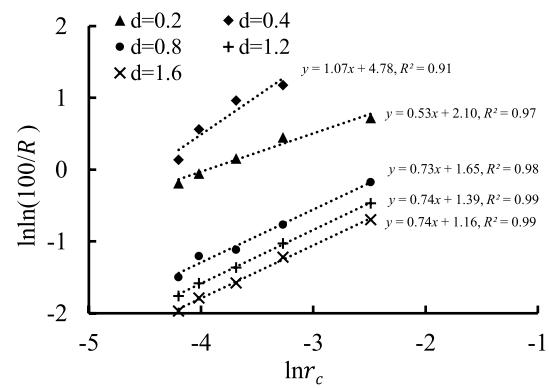


Fig. 7 The fitted curves of the Rosin–Rammler equation in log–log coordinates ( $v = 16$  mm/s,  $\theta = 20^\circ$ )

and  $\ln r_c$  (all the correlation coefficients are above 0.9). In other words, the distribution of cuttings size conforms to the Rosin–Rammler equation. In addition, the calculated  $n_b$  and  $r_e$  are given in “Appendix.”

As shown in Fig. 8, the absolute grain size of the cuttings ( $r_e$ ) increases with an increased DOC, but these changes gradually reach a plateau. Considering the relationship between the MSE and DOC, there is reason to believe the quantitative correlation between the MSE and  $r_e$ . As shown in Fig. 9, the correlation between MSE and  $r_e$  was found to be in the form of exponential. This shows that the absolute grain size ( $r_e$ ) can be an indicator of cuttings size in this context, however, it is not practical because the calculation of  $r_e$  is complex, and the distribution of cuttings size may not conform to the Rosin–Rammler equation under other rock cutting conditions.

#### 3.2.2 Mass fraction changes of cuttings of different sizes

The cuttings produced during rock cutting vary in size, so it is necessary to collect them and divide them into several groups

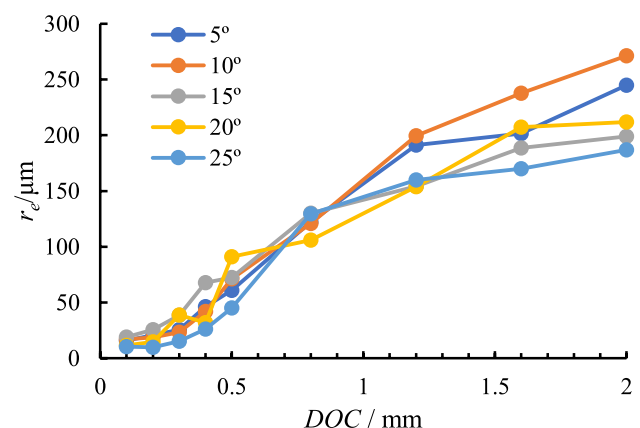


Fig. 8 Relationship between  $r_e$  and the depth of cut

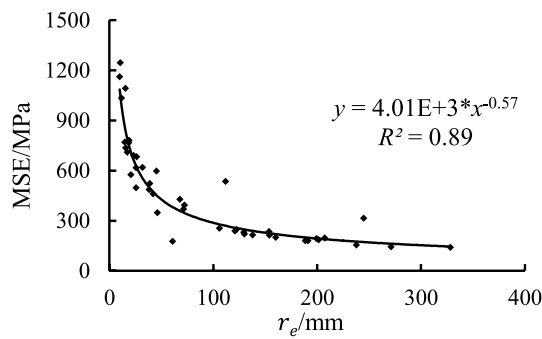


Fig. 9 Relationship between MSE and  $r_e$

using sieves to complete this research. From this process, the mass fraction of each group was calculated, and its variation with the back rake angle and depth of cut were discussed.

Figure 10 shows the mass fraction changes of cuttings of different sizes with the back rake angle when the depth of cut is 0.5 mm. As can be seen from Fig. 10, the mass fraction of the cuttings with sizes between 150 and 200  $\mu\text{m}$  (80–100 mesh) is the lowest regardless of the back rake angle. As the back rake angle increases, the mass fraction of cuttings smaller than 180  $\mu\text{m}$  (100 mesh) increases from 25.8 to 34.3%, but the mass fraction of cuttings larger than 840  $\mu\text{m}$  (20 mesh) increases slightly and reaches a maximum ( $\theta = 15^\circ$ ) and then decreases sharply. This phenomenon suggests that chunk-like cuttings decrease, but powder-like cuttings increase as the back rake angle increases. One reason is that the normal force applied to the surface of rock increases as back rake angle increases, then more rock in front of the cutter broken into smaller cuttings by compression [19]. Another reason is that some of the cuttings which were produced could not escape from the space between the cutter and the rock because this space becomes smaller as the back rake angle increases. These cuttings could then suffer secondary breakage to form smaller cuttings.

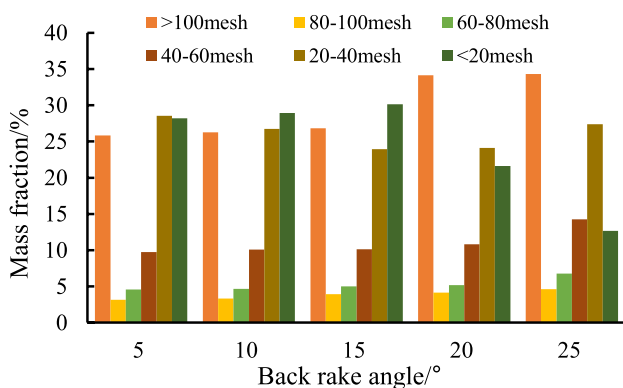


Fig. 10 Mass fraction changes with back rake angle (DOC=0.5 mm)

Furthermore, the mass fraction changes with the depth of cut, when the back rake angle is  $25^\circ$ , are shown in Fig. 11, as the depth of cut increases from 0.1 to 2 mm, the mass fraction of cuttings smaller than 180  $\mu\text{m}$  (100 mesh) has dropped from about 80% to less than 15%, but against this, the mass fraction of cuttings larger than 830  $\mu\text{m}$  (20 mesh) has increased from 0% to about 70%. Beyond that, as the depth of cut increases, the mass fraction of cuttings of size smaller than 250  $\mu\text{m}$  (60 mesh) decreased sharply, but the mass fraction of cuttings with sizes between 420 and 830  $\mu\text{m}$  (20–40 mesh) increased dramatically, and the mass fraction of cuttings with sizes between 250 and 420  $\mu\text{m}$  (40–60 mesh) increases first and then decreases. These results show that as the depth of cut increased, the mass fraction of larger cuttings increased while the mass fraction of smaller cuttings decreased. The depth of cut can significantly influence cuttings size. This maybe because the cracks inside rock propagated deeply and the rock failure mode changed from ductile-dominated mode to brittle-dominated mode as the depth of cut increased [15, 19].

However, the mass fractions of cuttings of different sizes cannot indicate cuttings size in the quantitative research so the CI was selected as the indicator of cuttings size.

### 3.2.3 The relationship between the MSE and cuttings size

The reason to use CI as the indicator of cuttings size is that CI is easy to calculate, as discussed in Sect. 2.2. Figure 12 shows the influence of depth of cut on the CI value. The CI value increased with increasing depth of cut, which is consistent with previous researches [22, 32]. It is observed from Fig. 8 that  $r_e$  also increased with the increase of depth of cut, which means with the depth of cut increased, the mass fraction of larger cuttings increased. Figures 8 and 12 also indicate a significant relationship between CI and  $r_e$ , which is similar to the research results of Heydari [23]. The relationship of the MSE with CI value was investigated, as seen in Fig. 13, the MSE decreased with increasing CI for different

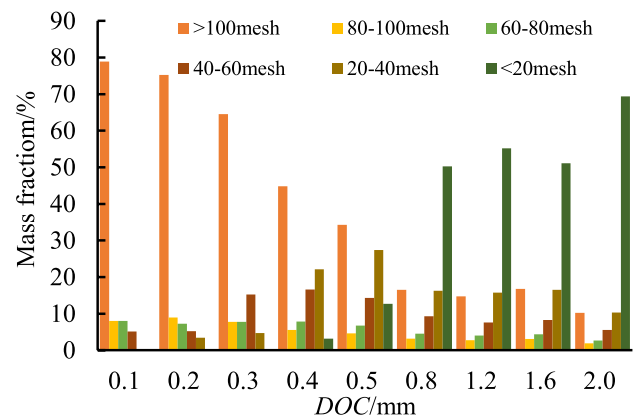


Fig. 11 Mass fraction changes with depth of cut ( $\theta = 25^\circ$ )

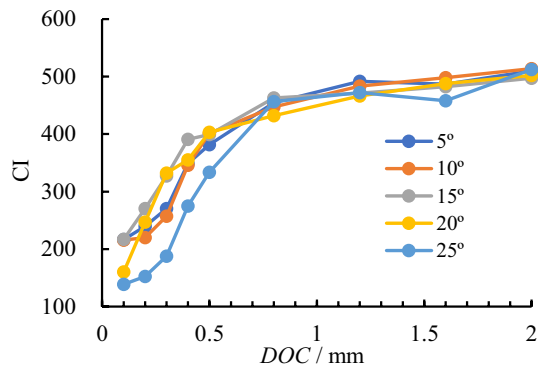


Fig. 12 Relationship between CI and depth of cut

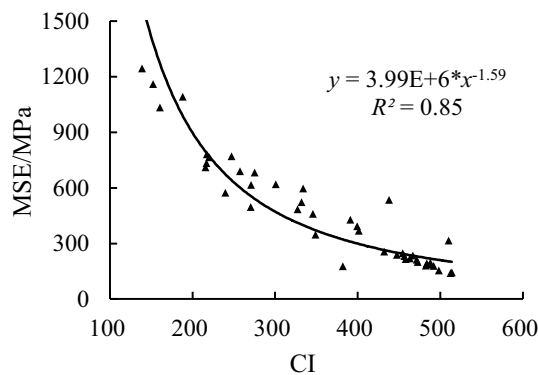


Fig. 13 Relationship between MSE and CI

cutting parameters. In other words, the cutting efficiency increased with increasing CI, which shows that the CI could be an indicator of rock cutting efficiency. The correlation between the MSE and CI was found to be  $MSE = kCI^n$ , as given in Fig. 13. This result could provide new way to monitoring the drilling efficiency at construction site.

The surface energy principle can explain these phenomena. That is, in the cutting process, the energy consumption is proportional to the area of the new surface created. When the depth of cut is shallow, new cracks inside the rock cannot propagate to the free surface, so most of the cuttings are powder-like, and the area of the newly formed surface is large in the unit volume of rock, so the MSE is large. On the contrary, when the depth of cut is deep, chunk-like cuttings are formed because some new cracks inside the rock

propagate to free surface and the MSE decreases with the decrease of the area of the newly formed surface in the unit volume of rock.

## 4 The effects of cutting parameters on the MSE and cuttings size

### 4.1 Experimental design

To analyze the effects of the cutting parameters ( $\theta$ , DOC, and  $v$ ) on the value of the MSE and the CI, the Taguchi method was used in this research. The Taguchi method is one of the statistical methods that reduces the number of experiments and assesses the influence of each parameter on the results [33]. Therefore, using the Taguchi method led to a significant reduction in the time and cost of rock cutting tests. In these tests, depth of cut, back rake angle and cutting speed were selected as the input parameters. A 5-level and 3-factor L25 OA was used to design the tests. The selected parameters and their levels are shown in Table 4, and the experimental layout is shown in Table 5.

In this section, the MSE and CI values were selected as the response factor, and the results of the cutting tests are also shown in Table 5. Using Design-expert software, the effects of cutting parameters on responses were analyzed, and each parameter’s contribution to the response was obtained using ANOVA method.

### 4.2 Results and discussion

#### 4.2.1 Cutting parameters effects on MSE and CI

The effects of the three main cutting parameters (depth of cut, back rake angle and cutting speed) on the MSE and CI are shown in Figs. 14 and 15. In Fig. 14, the MSE decreases with the increased depth of cut, but the decrease is gradually reduced. This trend was supported by previous work by Richard [11], Zhou [13] and He [14, 15]. Similar to the work of Rajabov [25], the MSE increased slightly with the increase in back rake angle. However, the cutting speed effect on the MSE is difficult to assess. As shown in Fig. 15, the CI value increased when the depth of cut increased from 0.3 to 1.5 mm, and the CI value decreased slightly with the

Table 4 Cutting parameters and their levels

Symbol	Parameters	Level of factors				
		1	2	3	4	5
A	Depth of cut ( <i>DOC</i> , mm)	0.3	0.6	0.9	1.2	1.5
B	Back rake angle ( $\theta$ , °)	5	10	15	20	25
C	Cutting speed ( $v$ , mm/s)	4	8	12	16	20

**Table 5** Experiment layout and results

Test No	A	B	C	MSE (MPa)	CI
1	1	1	1	263.41	370.53
2	1	2	2	288.91	406.47
3	1	3	3	505.51	340.21
4	1	4	4	442.58	359.19
5	1	5	5	684.35	301.92
6	2	1	2	272.45	422.82
7	2	2	3	372.75	394.67
8	2	3	4	279.44	446.55
9	2	4	5	381.63	390.93
10	2	5	1	301.84	416.73
11	3	1	3	227.41	469.70
12	3	2	4	229.27	467.52
13	3	3	5	259.46	452.69
14	3	4	1	255.21	449.08
15	3	5	2	294.13	448.15
16	4	1	4	205.19	194.66
17	4	2	5	194.67	478.47
18	4	3	1	187.23	487.42
19	4	4	2	251.98	459.21
20	4	5	3	302.57	455.36
21	5	1	5	184.85	494.55
22	5	2	1	144.09	503.49
23	5	3	2	192.32	484.51
24	5	4	3	225.35	473.86
25	5	5	4	250.12	465.44

increased back rake angle. However, within the range of the experiments, the cutting speed had no obvious impact on the CI value. These results also showed a strong inverse

correlation between the MSE and the cuttings size indicator (CI).

These results are easy to understand by considering the mechanism of rock breaking. According to Fig. 16a, when the cutting depth is shallow, a small part of the rock is crushed along with the nominal cracks formed at the tip of the cutter, eventually forming powder-like cuttings. Because the cracks could not reach to the free surface to form chips, the cuttings size is small. Conversely, when the cutting depth is deep, except for the formation of powder-like cutting at the tip of the cutter, some cracks could reach to the free surface to form chips, as shown in Fig. 16b, resulting in a larger cuttings size than when the cutting depth is shallow. The larger the cuttings are, the more new surfaces are formed during rock cutting, the more energy is needed to break the rock, the higher the MSE is.

Rock cutting with a small back rake angle and a large back rake angle is shown in Fig. 17. When all other parameters are the same, the normal force applied to the rock increases with an increased back rake angle. As a result, more of the rock is crushed and forms more powder-like cuttings, causing a decrease in the CI value. Another possible reason is that an increase in the back rake angle caused more rock failures in ductile-mode [14], which leads to decreasing cuttings size. However, compared to the depth of cut, the back rake angle has lesser impact on the MSE and cuttings size in these tests, which is shown in Figs. 14b and 15b.

**4.2.2 Analysis of variance (ANOVA)**

ANOVA is an analysis tool used to study the statistically significant parameters that influence the quality characteristics and to identify the contribution ratio of each process

**Fig. 14** Mean effects plot for mean MSE

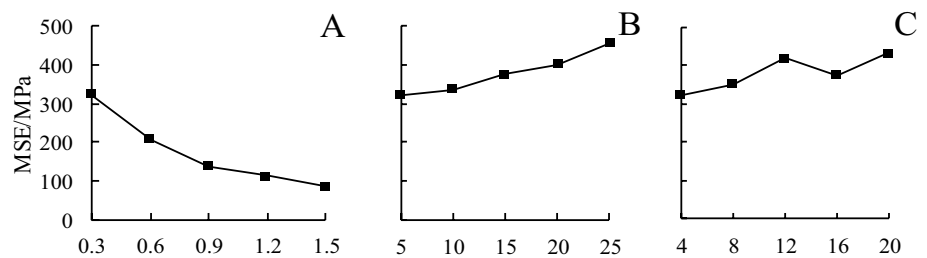
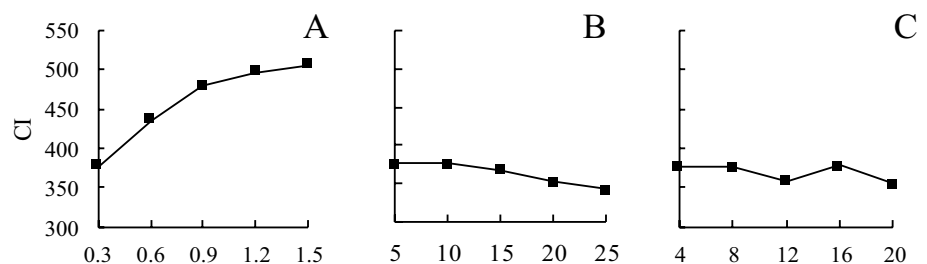


**Fig. 15** Mean effects plot for mean CI





factor on the responses. In the ANOVA table, the sum of squares is obtained by computing the sum of the squared differences between the average values for the blocks and the overall mean. The mean square is calculated by the block sum of squares divided by the block degrees of freedom. The F-value is calculated by the mean square divided by the residual mean square, and the P-value is determined from the F-value. If the P-value is very small (less than 0.05) then the terms in the model significantly affect the response (confidence level 95%).

The results of ANOVA for MSE and CI are presented in Tables 6 and 7, respectively. It can be seen from Table 6 that the depth of cut and back rake angle are the statistically significant factors influencing the MSE since the *P* values of these factors are less than 0.05. Compared to these factors, cutting speed has no impact on the MSE. Table 6 also indicates that the most influential factor for the MSE is depth

of cut (contribution 54.9%), followed by the back rake angle (contribution 18%). In Table 7, it can be seen that depth of cut and back rake angle have a significant impact on the CI value, and the most influential factor on the CI value is the depth of cut (contribution 84.1%), followed by the back rake angle (contribution 6.5%). Cutting speed (contribution 3.7%) has an insignificant effect on CI value.

## 5 Conclusions

In this paper, several linear rock cutting tests were conducted to study the relationship between mechanical specific energy and cuttings size. Also, the resulting cuttings size distribution was discussed. After selecting the CI as the best indicator of cuttings size, rock cutting tests based on the Taguchi's method were conducted to analyze the effects of the cutting

**Fig. 16** Rock cutting at **a** shallow depth, **b** large depth

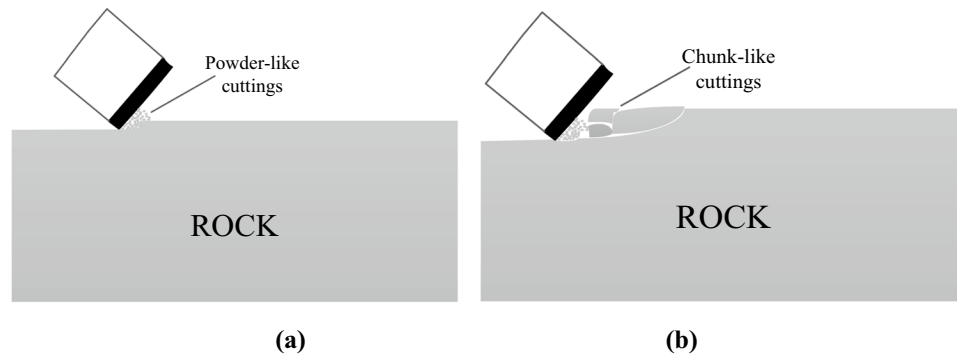


**Fig. 17** Rock cutting with **a** small back rake angle, **b** large back rake angle

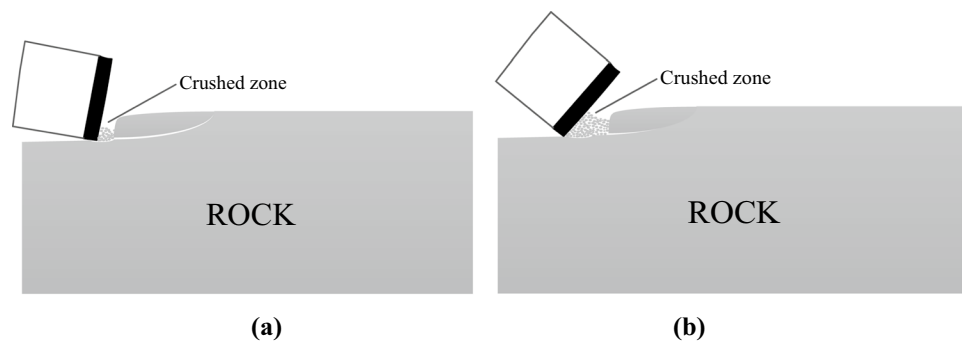


**Table 6** Results of ANOVA for MSE

Parameters	Sum of squares	DF	Mean square	F value	P-value	Contribution (%)
Model	$2.8 \times 10^5$	12	$2.34 \times 10^4$	6.05	0.002	
Depth of cut	$1.80 \times 10^5$	4	$4.50 \times 10^4$	11.61	0	54.9
Back rake angle	$5.90 \times 10^4$	4	$1.47 \times 10^4$	3.81	0.03	18.0
Cutting speed	$4.23 \times 10^4$	4	$1.06 \times 10^4$	2.73	0.08	13.0
Residual	$4.65 \times 10^4$	12	$3.87 \times 10^3$			
Total	$3.28 \times 10^5$	24				

**Table 7** Results of ANOVA for CI

Parameters	Sum of squares	DF	Mean square	F value	P-value	Contribution (%)
Model	$6.30 \times 10^4$	12	$5.25 \times 10^3$	17.02	0	
Depth of cut	$5.62 \times 10^4$	4	$1.40 \times 10^4$	45.51	0	84.1
Back rake angle	$4.36 \times 10^3$	4	$1.09 \times 10^3$	3.53	0.04	6.5
Cutting speed	$2.49 \times 10^3$	4	$6.23 \times 10^2$	2.02	0.16	3.7
Residual	$3.70 \times 10^3$	12	$3.09 \times 10^2$			
Total	$6.67 \times 10^4$	24				

parameters ( $\theta$ , DOC, and  $\nu$ ) on cuttings size and the MSE. The main conclusions obtained from these experiments may be summarized as follows:

1. The distribution of cuttings size conforms to the Rosin–Rammler equation. When fitted using a linear regression method, all the correlation coefficients of the fitted curves are above 0.9.
2. There is a strong inverse correlation between cuttings size and MSE. The quantitative analysis based on 45 sets of experimental results indicates that the relationship between MSE and CI (or  $r_e$ ) could be described as an exponential function.
3. For both the MSE and the CI, the most influential factor is the depth of cut, the MSE decreases with increased depth of cut, but the CI value increases with increased

depth of cut. ANOVA results show that the contributions of the depth of cut for MSE and the CI are 54.9% and 84.1%, respectively.

4. The back rake angle also has a significant impact on the MSE and the CI value. The MSE decreases slightly with increased back rake angle, and the CI value increases slightly with increased back rake angle. However, it does not make as great a contribution as the depth of cut for the MSE and the CI value (18% and 6.5%, respectively).
5. Within the range of the experiment, cutting speed (from 4 to 20 mm/s) has an insignificant effect on the MSE and the CI value.

This work is highly pertinent to a better understanding of the relationship between rock cutting efficiency and cuttings size during rock cutting using a PDC cutter.

## Appendix: The results of the experiments in Section 3

$\theta$ (°)	DOC (mm)	Cuttings weight (mg)						Parameters of Rosin–Rammler equation			CI
		<20	20–40	40–60	60–80	80–100	>100	$n_b$	$r_e$	$R^2$	
		(mesh)	(mesh)	(mesh)	(mesh)	(mesh)	(mesh)	(mm)	(mm)		
5	0.1	0.8	6.1	2.4	3.2	2.8	23.1	0.66	0.016	0.97	216.67
	0.2	1.4	13.4	14.3	6.4	4.8	46.6	10.99	0.021	0.99	239.46
	0.3	4.3	23.2	18.8	8.4	6.0	52.9	0.97	0.026	0.99	239.46
	0.4	37.7	65.4	23.3	10.4	7.6	76.0	0.83	0.046	0.98	270.25
	0.5	124.4	140.8	48.1	22.5	15.5	142.2	0.81	0.046	0.98	348.91
	0.8	191.5	80.35	33.2	16.4	11.7	68.3	0.80	0.122	0.99	454.49
	1.2	378.1	101.2	42.0	20.2	13.6	76.8	0.80	0.191	0.99	491.78
	1.6	427.6	99.5	48.6	24.7	16.8	93.5	0.74	0.201	0.99	486.71
	2.0	422.9	85.8	38.8	17.6	11.3	63.1	0.81	0.245	0.99	509.86

$\theta(^{\circ})$	DOC (mm)	Cuttings weight (mg)						Parameters of Rosin–Rammler equation			CI
		<20	20–40	40–60	60–80	80–100	>100	$n_b$	$r_e$	$R^2$	
		(mesh)	(mesh)	(mesh)	(mesh)	(mesh)	(mesh)		(mm)		
10	0.1	0	7.3	7.6	4.2	3.0	32.8	0.84	0.017	0.99	215.42
	0.2	0.2	8.1	10.9	6.7	5.3	39.2	1.17	0.019	0.99	220.01
	0.3	1.1	18.6	16.4	8.0	5.5	46.0	1.13	0.023	0.98	257.40
	0.4	20.7	61.0	21.8	9.9	6.9	58.7	0.98	0.042	0.97	345.62
	0.5	75.9	70.2	26.5	12.3	8.7	68.9	0.82	0.068	0.99	394.53
	0.8	213.7	90.9	35.9	18.7	13.8	85.2	0.76	0.121	0.99	447.26
	1.2	461.2	107.3	53.4	27.2	19.1	106.2	0.73	0.199	0.99	483.39
	1.6	668.5	131.3	65.5	34.7	22.4	121.4	0.75	0.238	0.99	498.20
15	0.1	0	2.5	3.7	5.7	3.8	15.3	1.39	0.019	0.98	217.10
	0.2	2.8	18.7	13.7	8.4	6.5	39.7	1.03	0.026	0.99	270.60
	0.3	18.2	37.3	20.2	9.6	6.6	51.9	0.89	0.038	0.99	327.12
	0.4	43.7	58.4	24.1	12.5	9.5	67.3	0.84	0.050	0.99	359.41
	0.5	79.7	63.4	26.8	13.3	10.5	71.0	0.78	0.068	0.99	390.76
	0.8	238.6	90.5	40.7	18.8	13.8	73.8	0.82	0.130	0.99	462.98
	1.2	391.9	116.0	58.2	27.7	20.0	106.6	0.78	0.154	0.99	471.19
	1.6	554.6	133.1	67.9	33.7	24.7	127.8	0.75	0.189	0.99	482.39
20	0.1	0	1.4	1.2	3.6	5.2	24.5	1.07	0.012	0.99	160.17
	0.2	8.0	5.0	6.4	4.8	3.1	35.2	0.70	0.015	0.99	246.92
	0.3	30.9	47.3	22.0	11.3	8.2	70.2	0.78	0.039	0.99	331.95
	0.4	12.6	38.8	17.7	9.2	7.1	62.4	0.87	0.032	0.98	300.61
	0.5	48.2	53.7	24.1	11.6	9.3	76.1	0.75	0.050	0.99	351.44
	0.8	219.1	100.7	46.7	10.6	3.0	101.8	0.74	0.106	0.98	432.02
	1.2	409.0	125.1	57.7	30.5	20.9	121.1	0.75	0.154	0.99	466.39
	1.6	598.0	125.1	67.7	32.5	23.1	128.5	0.74	0.207	0.99	488.02
25	0.1	0	0	1.4	2.2	2.2	21.7	1.26	0.010	0.99	138.76
	0.2	0	1.2	1.8	2.5	3.1	26.1	0.93	0.010	0.94	152.24
	0.3	0	3.0	9.8	5.0	5.0	41.4	1.07	0.015	0.98	187.85
	0.4	4.3	30.0	22.5	10.6	7.5	60.8	1.03	0.026	0.99	275.02
	0.5	24.3	52.5	27.4	13.0	8.9	65.8	0.93	0.040	0.99	333.78
	0.8	290.0	93.5	53.6	26.2	18.0	95.4	0.78	0.129	0.99	456.44
	1.2	455.1	129.6	62.8	33.3	22.7	121.6	0.76	0.160	0.99	472.30
	1.6	461.9	149.2	74.7	39.0	27.7	151.5	0.75	0.138	0.99	457.97
	2.0	1238.6	184.1	99.1	48.0	33.2	182.0	0.71	0.328	0.99	512.12

1. CI is coarseness index,  $R^2$  is the correlation coefficient of the fitted curves of Rosin–Rammler equation. 2. Rosin–Rammler equation:  $R = 100\exp(-(r_c/r_e)^{n_b})$ , where  $R$  is the cumulative fraction of cuttings by weight retained on the sieve that of mesh size  $r_c$ ,  $r_e$  is the absolute grain size,  $n_b$  is a constant describing the uniformity of the cuttings.

**Acknowledgements** This work was supported by National Natural Science Foundation of China (Grant No. 51874327) and Scientific Research Starting Foundation of China University of Petroleum-Beijing at Karamay (RCYJ2016B-02-004).

## References

- Bellin F, Dourfaye A, King W, Thigpen M (2010) The current state of PDC bit technology. *World Oil* 231(11):67–71
- Chen L, Yang YX, Liu Y, Lin M, Zhang CL, Niu SW (2017) The operational theory and experimental study of scraping-wheel diamond bit. *J Petrol Sci Eng* 156:152–159
- Iman R, Babak A, Brian E (2018) Analysis of rock cutting process with a blunt PDC cutter under different wear flat inclination angles. *J Petrol Sci Eng* 171:771–783
- Caicedo HU, Calhoun WM, Ewy RT (2005) Unique ROP predictor using bit-specific coefficient of sliding friction and mechanical

- efficiency as a function of confined compressive strength impacts drilling performance. In: SPE/IADC drilling conference and exhibition, Feb 23–25, Amsterdam, The Netherlands
5. Hareland G, Yan W, Nygaard R, Wise JL (2009) Cutting efficiency of a single PDC cutter on hard rock. *J Can Pet Technol* 48(6):60–65
  6. Liu W, Zhu X (2019) A new approach of rock cutting efficiency evaluation by using plastic energy dissipation ratio. *KSCE J Civ Eng* 23(2):879–888
  7. Wang X, Wang Z, Wang D, Chai L (2018) A novel method for measuring and analyzing the interaction between drill bit and rock. *Measurement* 121:344–354
  8. Teale R (1965) The concept of specific energy in rock drilling. *Int J Rock Mech Min Sci Geomech Abstr* 2(2):57–73
  9. Chen P, Meng M, Miska S, Yu M, Ozbayoglu E, Takach N (2019) Study on integrated effect of PDC double cutters. *J Pet Sci Eng* 178:1128–1142
  10. Thomas GB, Steven CF (1991) Specific grinding energy as an in-process control variable for ductile-regime grinding. *Precis Eng* 13(4):256–262
  11. Richard T (1999) Determination of rock strength from cutting tests. University of Minnesota, Minneapolis
  12. Richard T, Dagrain F, Poyol E, Detournay E (2012) Rock strength determination from scratch tests. *Eng Geol* 147–148:91–100
  13. Zhou Y, Lin JS (2013) On the critical failure mode transition depth for rock cutting. *Int J Rock Mech Min Sci* 62:131–137
  14. He X, Xu C, Peng K, Huang G (2017) On the critical failure mode transition depth for rock cutting with different back rake angles. *Tunn Undergr Space Technol* 63(3):95–105
  15. He X, Xu C (2016) Specific energy as an index to identify the critical failure mode transition depth in rock cutting. *Rock Mech Rock Eng* 49(4):1461–1478
  16. Hong J, Fan X, Liu Y, Liu G, Liu B, Talalay P (2015) Size distribution and shape characteristics of ice cuttings produced by an electromechanical auger drill. *Cold Reg Sci Technol* 119(11):204–210
  17. Rispoli A, Ferrero AM, Cardu M, Farinetti A (2017) Determining the particle size of debris from a tunnel boring machine through photographic analysis and comparison between excavation performance and rock mass properties. *Rock Mech Rock Eng* 50:2805–2816
  18. Akbari B, Miska S, Yu M, Ozbayoglu E (2014) Relation between the mechanical specific energy, cuttings morphology, and PDC cutter geometry. In: Proceedings of the ASME 2014 33rd international conference on ocean, offshore and arctic engineering. Materials technology; petroleum technology, vol 5. June 8–13, San Francisco, California, USA
  19. Zhen C, Mao S, Gensheng L, Zhongwei H, Xiaoguang W, Zhaopeng Z, Jiawei Y (2018) Imaging the formation process of cuttings: characteristics of cuttings and mechanical specific energy in single PDC cutter tests. *J Pet Sci Eng* 171:854–862
  20. Hughes HM (1986) The relative cuttability of coal-measures stone. *Min Sci Technol* 3(2):95–109
  21. Tuncdemir H, Bilgin N, Copur H, Balci C (2008) Control of rock cutting efficiency by muck size. *Int J Rock Mech Min Sci* 45(2):278–288
  22. Roxborough FF, Rispin A (1973) The mechanical cutting characteristics of the lower chalk. *Tunn Tunn Int* 5:45–67
  23. Heydari S, Hamidi JK, Monjezi M, Eftekhari A (2019) An investigation of the relationship between muck geometry, TBM performance, and operational parameters: a case study in golab II water transfer tunnel. *Tunn Undergr Space Technol* 88(1):73–86
  24. Che D, Zhang W, Ehmann K (2017) Chip formation and force responses in linear rock cutting: an experimental study. *J Manuf Sci Eng* 139(1):011011
  25. Rajabov V, Miska SZ, Mortimer L, Yu MJ, Ozbayoglu ME (2012) The effects of back rake and side rake angles on mechanical specific energy of single PDC cutters with selected rocks at varying depth of cuts and confining pressures. In: IADC/SPE drilling conference and exhibition, Mar 6–8, San Diego, California, USA
  26. Menezes PL (2017) Influence of cutter velocity, friction coefficient and rake angle on the formation of discontinuous rock fragments during rock cutting process. *Int J Adv Manuf Technol* 90:3811–3827
  27. Rafatian N, Miska SZ, Ledgerwood LW, Yu MJ, Ahmed R (2009) Experimental study of MSE of a single PDC cutter under simulated pressurized conditions. In: SPE/IADC drilling conference and exhibition, Mar 17–19, Amsterdam, The Netherlands
  28. Xia HN, Wang KX, Zhai YH, Cai JL (1997) Experimental research of PDC cutter shapes on breaking rock efficiency under various confining pressures. *J Jiangnan Pet Inst* 19:48–50 (in Chinese)
  29. Akbari B, Miska S, Mengjiao Y, Ozbayoglu E (2013) Effect of rock pore pressure on mechanical specific energy of rock cutting using single PDC cutter. In: 47th U.S. rock mechanics/ geomechanics symposium, June 23–26, San Francisco, California, USA
  30. Hegde C, Daigle H, Millwater H, Gray K (2017) Analysis of rate of penetration (ROP) prediction in drilling using physics-based and data-driven models. *J Pet Sci Eng* 159:295–306
  31. Rosin P, Rammler E (1933) The laws governing the fineness of powdered coal. *J Inst Fuel* 7:29–36
  32. Wang X (2017) Study on rock breaking mechanism using conical picks and cutting performance of roadheaders. Chongqing University, Chongqing (in Chinese)
  33. Javad S, Masoud G, Aliakbar A, Enayatolah D (2018) Optimisation of drilling parameters on St37 based on Taguchi method. *J Braz Soc Mech Sci Eng* 40:370

**Publisher's Note** Springer Nature remains neutral with regard to jurisdictional claims in published maps and institutional affiliations.